

Electronic Supporting Information (ESI)

Emissive Dual-Sensitized Bimetallic Eu₂^{III}-Bioprobe: Design Strategy, Biological Interactions, and Nucleoli Staining Studies

Usha Yadav,^a Madhu Verma,^b Zafar Abbas,^a Sri Sivakumar^b, and Ashis K. Patra^{a*}

^a *Department of Chemistry, Indian Institute of Technology Kanpur, Kanpur 208016, Uttar Pradesh, India*

^b *Department of Chemical Engineering and Centre for Environmental Science and Engineering, Indian Institute of Technology Kanpur, Kanpur 208016, Uttar Pradesh, India*

Table of contents	Page No.
Figure S1: ¹ H NMR (500 MHz, Chloroform- <i>d</i>) of [μ -pz(tpy) ₂] ligand (L)	3
Figure S2: ¹³ C NMR spectra (101 MHz, Chloroform- <i>d</i>) of [μ -pz(tpy) ₂] ligand (L)	4
Figure S3: ESI-MS spectra of [μ -pz(tpy) ₂] ligand (L)	4
Figure S4: FT-IR spectra of [Eu ₂ (tta) ₆ (μ -pz(tpy) ₂)] 1 and ligand L recorded in solid-state	5
Table S1: Selected FT-IR frequencies (in KBr disc) of Eu ₂ ^{III} -bioprobe and ligand L respectively	5
Table S2: Crystallographic data and structure refinement parameters of ligand L	6
Figure S5: Absorption spectra of tta and ligand L along with excitation spectra of Eu ₂ ^{III} -bioprobe 1	7
Figure S6: Time-dependent variations in absorption spectra of Eu ₂ ^{III} -bioprobe 1	8
Figure S7: UV-Vis spectral variations in Eu ₂ ^{III} -bioprobe 1 in different solvents	8
Figure S8: Steady-state luminescence spectra of the Eu ₂ ^{III} -bioprobe 1	9
Figure S9: Time-resolved luminescence spectral variations of Eu ₂ ^{III} -bioprobe 1 in the presence of different solvents	10
Table S3: Luminescence decay lifetime (τ) & rate constant (k) of the Eu ₂ ^{III} -bioprobe 1 in the different solvent system	10
Figure 10. (a) Absorption spectral traces of bridging ligand L with gradually increasing concentration of [CT-DNA] (b) Fluorescence emission spectral traces of EB-bound CT-DNA	11
Figure 11. (a) The effect of the addition of bridging ligand L in BSA solution (b) Modified Stern-Volmer plot of $\log [(I_0 - I)/I]$ vs. \log ligand L (c, d) Emission profile of synchronous emission spectra of BSA showing the quenching of emission after gradual addition of ligand L with $\Delta\lambda = 15$ nm and with $\Delta\lambda = 60$ nm	12

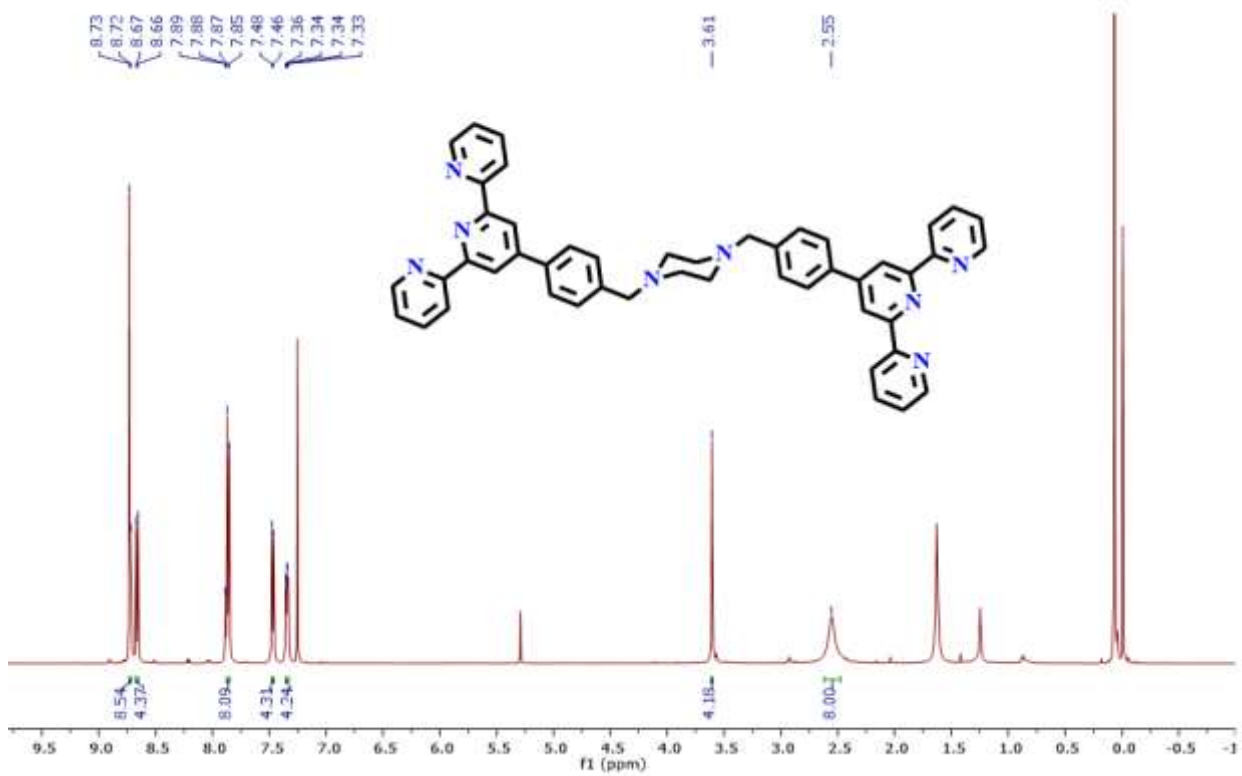


Figure S1: ¹H NMR (500 MHz, Chloroform-*d*) spectra of [μ-pz(tpy)₂] (L).

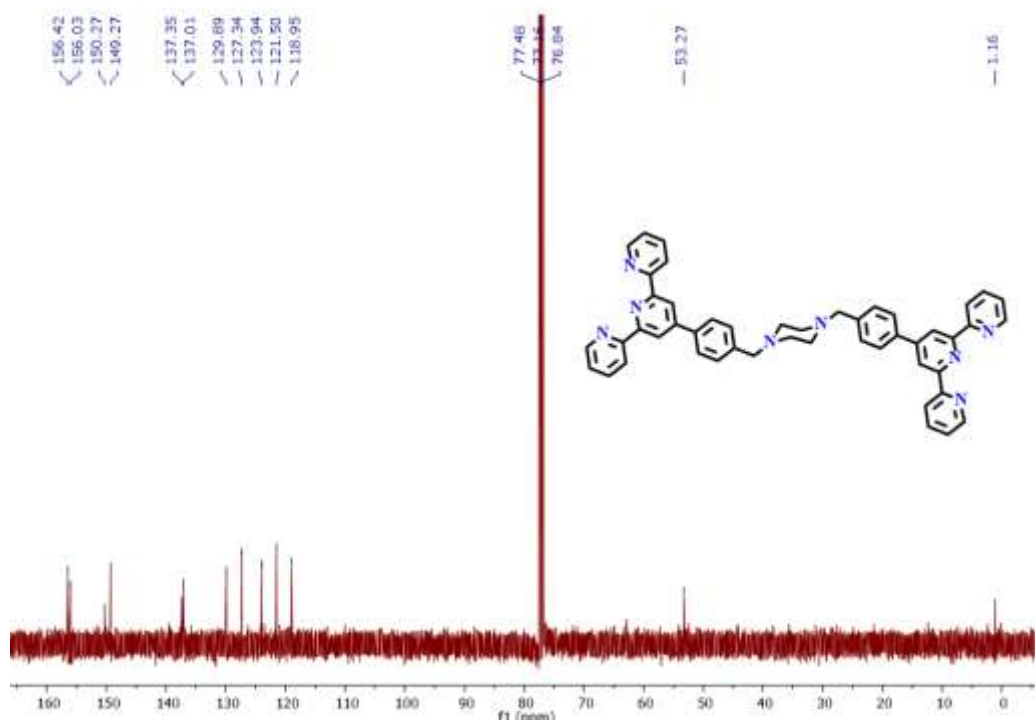


Figure S2: ^{13}C NMR spectra (101 MHz, Chloroform-*d*) spectra of $[\mu\text{-pz}(\text{tpy})_2] (\text{L})$.

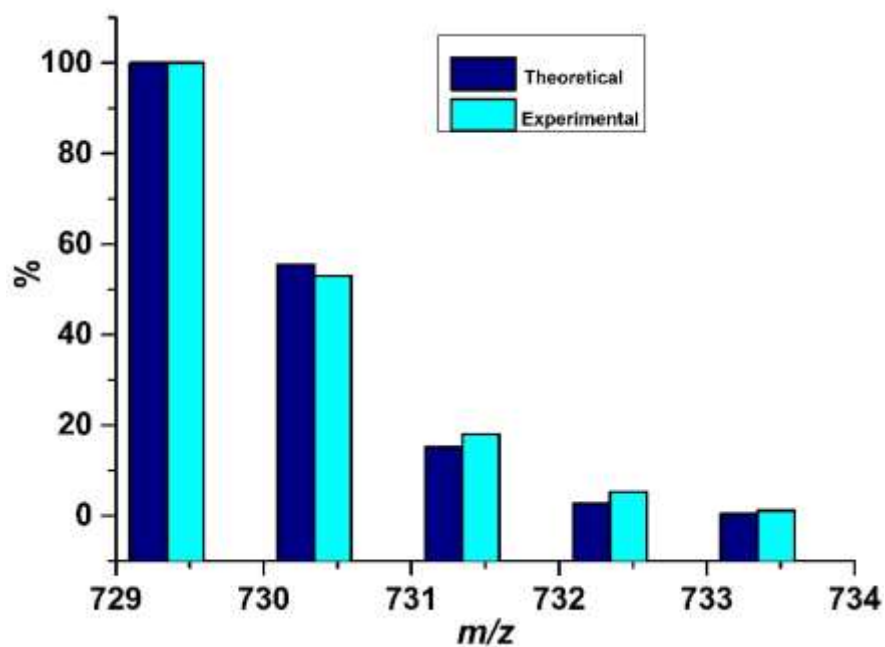


Figure S3: ESI-MS spectra of $[\mu\text{-pz}(\text{tpy})_2] (\text{L})$ showing their theoretical and experimental pattern.

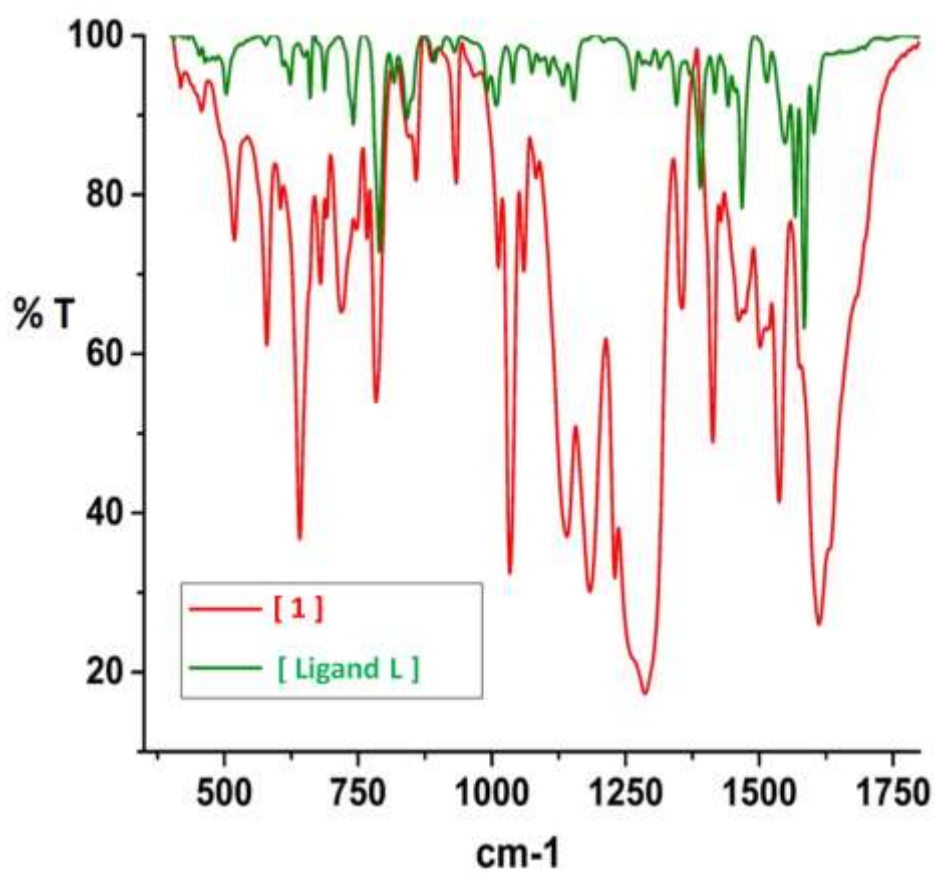


Figure S4: FT-IR spectra of Eu₂^{III}-bioprope (**1**) and [μ -pz(tpy)₂] (**L**) were recorded in solid-state.

Table S1: Selected FT-IR frequencies (KBr disc) of 1 and bridging ligand L		
($\bar{\nu}$ in cm ⁻¹)	[1]	[ligand L]
Eu-N	519	-
Eu-O	457	-
C-N	1183	1265
C=N	1428	1584
C=O	1611	-
C-F	1140	-

Table S2. Selected crystallographic data and structure refinement parameters of $[\mu\text{-pz}(\text{tpy})_2]$ (**L**) ligand.

Parameter	$[\mu\text{-pz}(\text{tpy})_2]$ ligand (L)
Empirical formula	C ₄₈ H ₄₀ N ₈
Formula weight	728.88
Crystal system	Monoclinic
Space group	<i>P</i> 2 ₁ / <i>c</i>
<i>a</i> Å	15.167(8)
<i>b</i> Å	8.833(5)
<i>c</i> Å	15.473(10)
α (deg)	90.00
β (deg)	118.39(3)
γ (deg)	90.00
Volume Å ³	1823.6(19)
<i>Z</i>	2
<i>D_x</i> (Mg m ⁻³)	1.327
μ (mm ⁻¹)	0.080
<i>F</i> (000)	768.0
<i>T</i> (K)	100(2)
θ range for data collection(deg)	2.766 to 28.874
Limiting indices	-20 ≤ <i>h</i> ≤ 20, -11 ≤ <i>k</i> ≤ 11, -20 ≤ <i>l</i> ≤ 20
Reflections collected	4511
Unique reflections	3180
<i>R</i> (int)	0.0573
<i>T</i> _{max} / <i>T</i> _{min}	0.746/0.690
Data/restraint/parameter	3180/0/253
GOF on <i>F</i> ²	1.033
<i>R</i> ₁ ^a and <i>wR</i> ₂ ^b [<i>I</i> > 2σ(<i>I</i>)]	0.0552 and 0.1321
<i>R</i> ₁ and <i>wR</i> ₂ (all data)	0.0877 and 0.1550
Largest diff. peak and hole (e.Å ⁻³)	0.33 and -0.29
CCDC deposition number	2129638

^a $R_1 = \sum ||F_0| - |F_c|| / \sum |F_0|$.

^b $wR_2 = \{ \sum [w(F_0^2 - F_c^2)] / \sum [w(F_0^2)] \}^{1/2}$

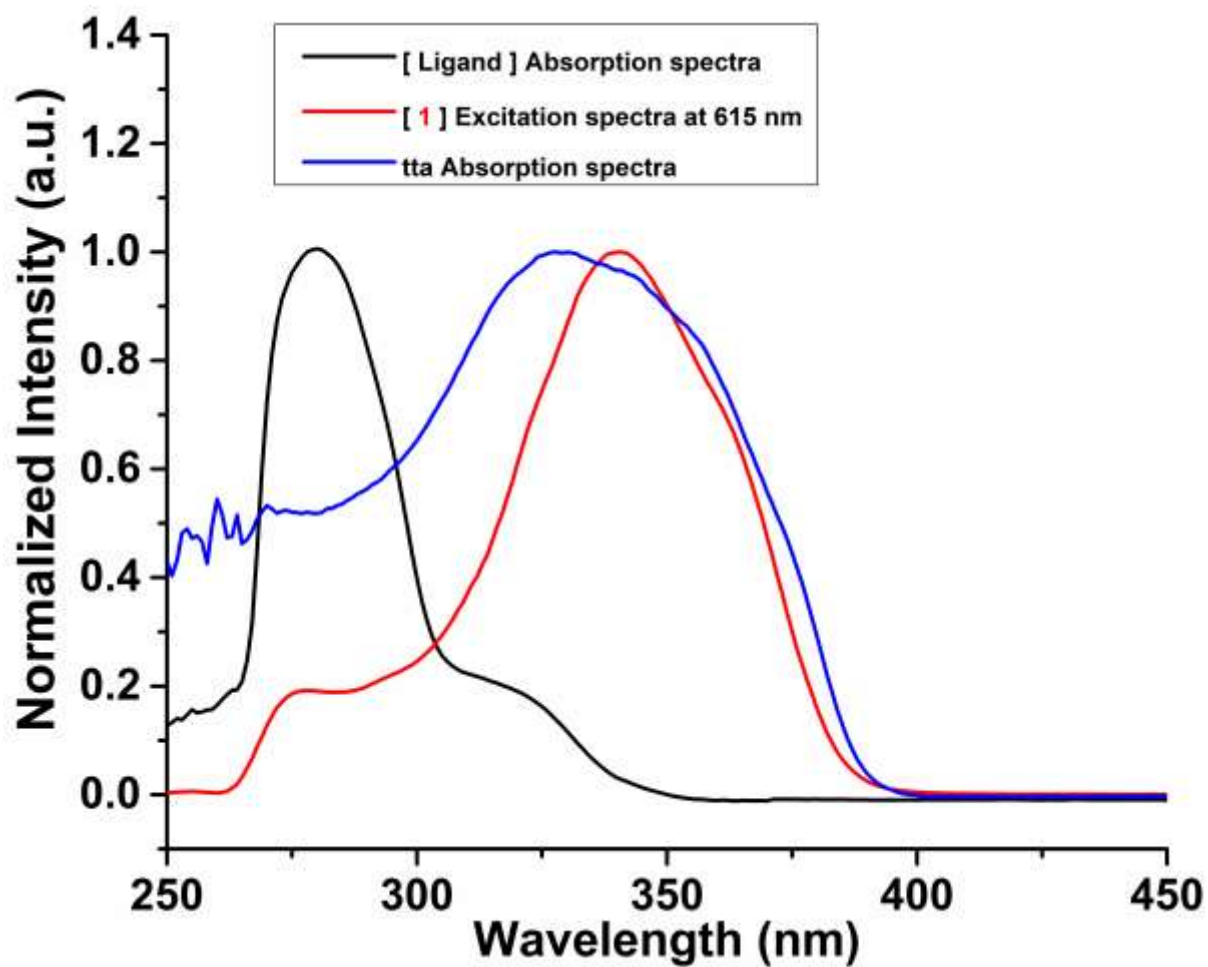


Figure S5: Absorption spectra of the bridging ligand L and tta along with the excitation spectra of Eu_2^{III} -bioprobe (**1**) in DMF. ($T = 298\text{K}$, $[\mathbf{1}] = 4 \mu\text{M}$, $[\text{tta}] = 20 \mu\text{M}$, $[\text{ligand L}] = 20 \mu\text{M}$. Ex. and Em. slit = $5 \times 5 \text{ nm}$)

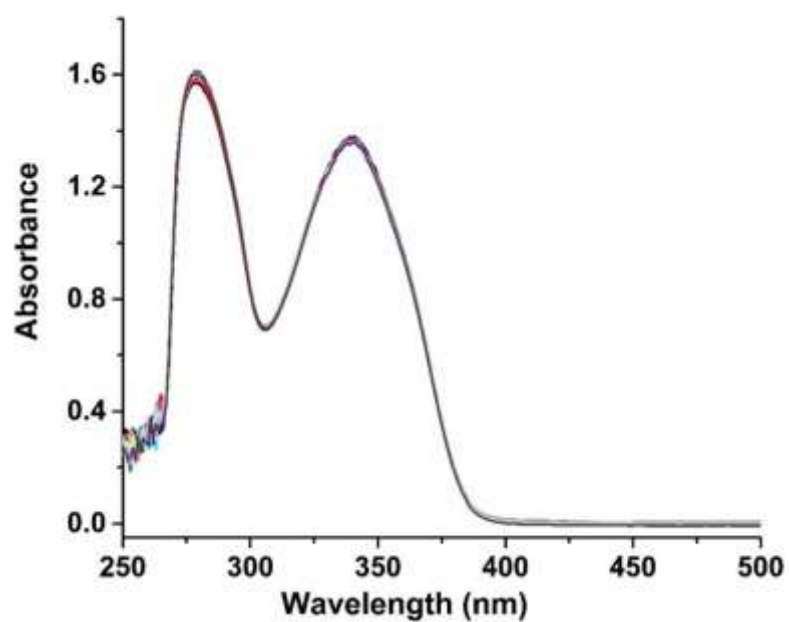


Figure S6: Time-dependent variations in absorption spectral of Eu_2^{III} -bioprobe (**1**) in DMF at 298 K for 4 h to access the stability of the respective complex in the solution-state. $[\mathbf{1}] = 20 \mu\text{M}$.

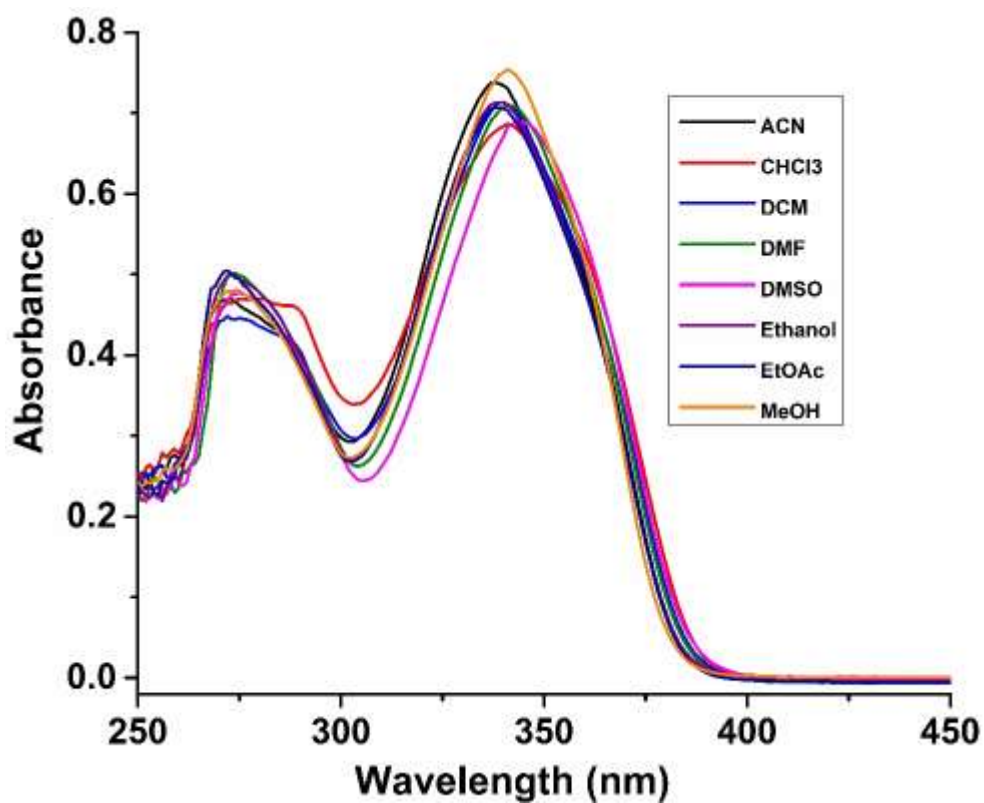


Figure S7: Solvent screening of Eu_2^{III} -bioprobe (**1**) in different solvents system using UV-Vis spectral study. ($T = 298 \text{ K}$, $[\mathbf{1}] = 10 \mu\text{M}$).

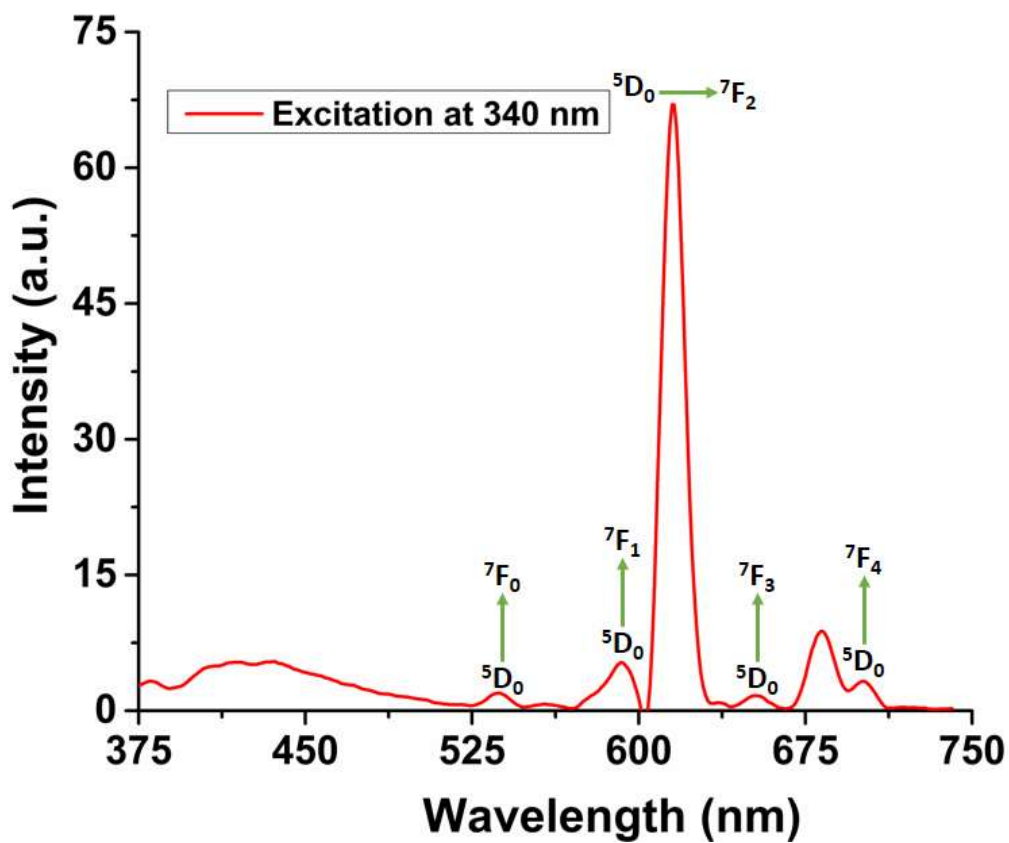


Figure S8: Steady state luminescence spectra of Eu²III-bioprobe **1** in DMF. (T= 298 K, $\lambda_{\text{ex}} = 340$ nm, $[\mathbf{1}] = 4 \mu\text{M}$, Ex. and Em. slit = 5×5 nm).

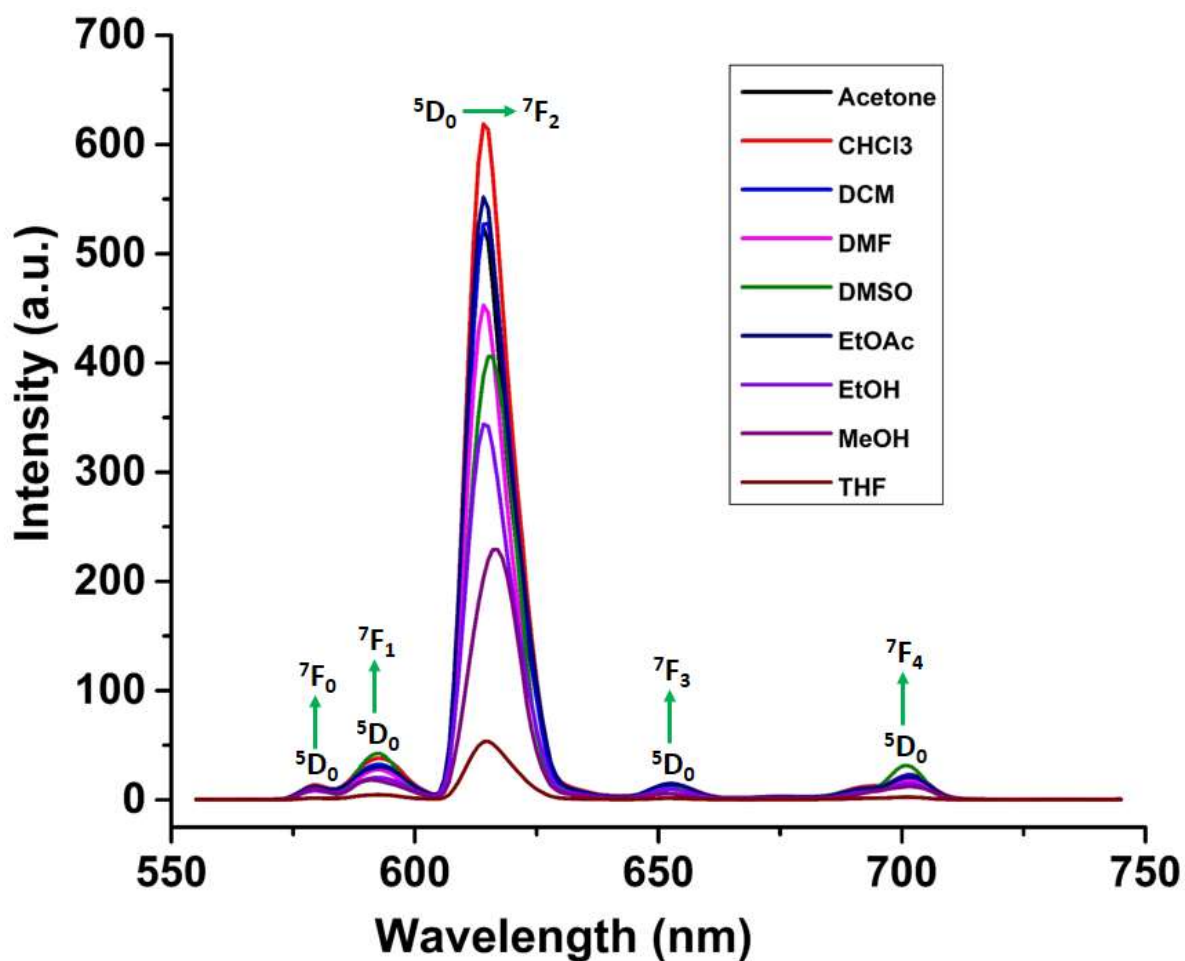


Figure S9: Time-resolved luminescence spectral variations of $\text{Eu}^{2\text{III}}$ -bioprobe (**1**) in the presence of different solvents showing the major changes in the spectral form ($T = 298 \text{ K}$, $\lambda_{\text{ex}} = 340 \text{ nm}$, $[\mathbf{1}] = 8 \mu\text{M}$, delay time = 0.2 (ms), and gate time = 0.2 (ms), Ex. and Em. slit= 2.5×5.0 respectively).

Table S3: Luminescence decay lifetime & rate constant of the complex in respective solvent system ($T = 298 \text{ K}$, $\lambda_{\text{ex}} = 340 \text{ nm}$, $[\mathbf{1}] = 8 \mu\text{M}$, delay time = 0.2 (ms), Ex. and Em. slit= 2.5×2.5 respectively)

Parameters	DMF	DMSO	MeOH	ACN	CHCl_3	EtOAc	THF	Acetone
$\tau(\text{ms})$	0.502	0.586	0.399	0.517	0.519	0.294	0.249	0.417
$\kappa(\text{s}^{-1})$	2.0	1.7	2.5	1.9	1.9	3.4	3.4	2.4

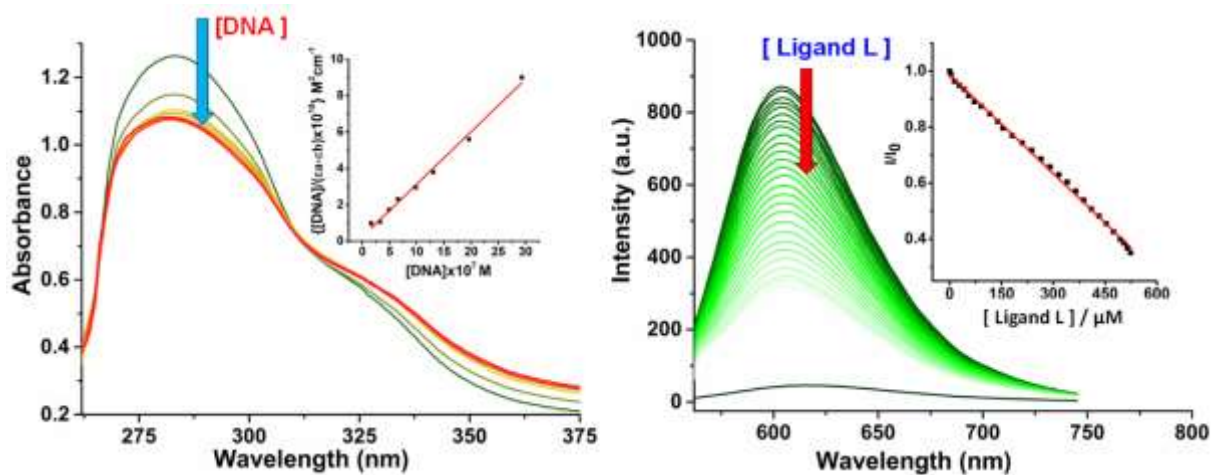


Figure S10. (a) Absorption spectral traces of $[\mu\text{-pz}(\text{tpy})_2]$ (**L**) with gradually increasing of [CT-DNA] in 5.0 mM Tris buffer (pH 7.2). Inset: $\Delta\lambda_{af}/\Delta\lambda_{bf}$ vs. [DNA] plot for ligand **L** (b) Fluorescence emission spectral traces of EB-bound CT-DNA with increasing concentration of ligand **L** in 5 mM Tris-buffer at $\lambda_{ex} = 546$ nm, $\lambda_{em} = 603$ nm, [EB] = 55 μM . Inset: plot shows the relative emission of I/I_0 vs. $[\mu\text{-pz}(\text{tpy})_2]$ (**L**).

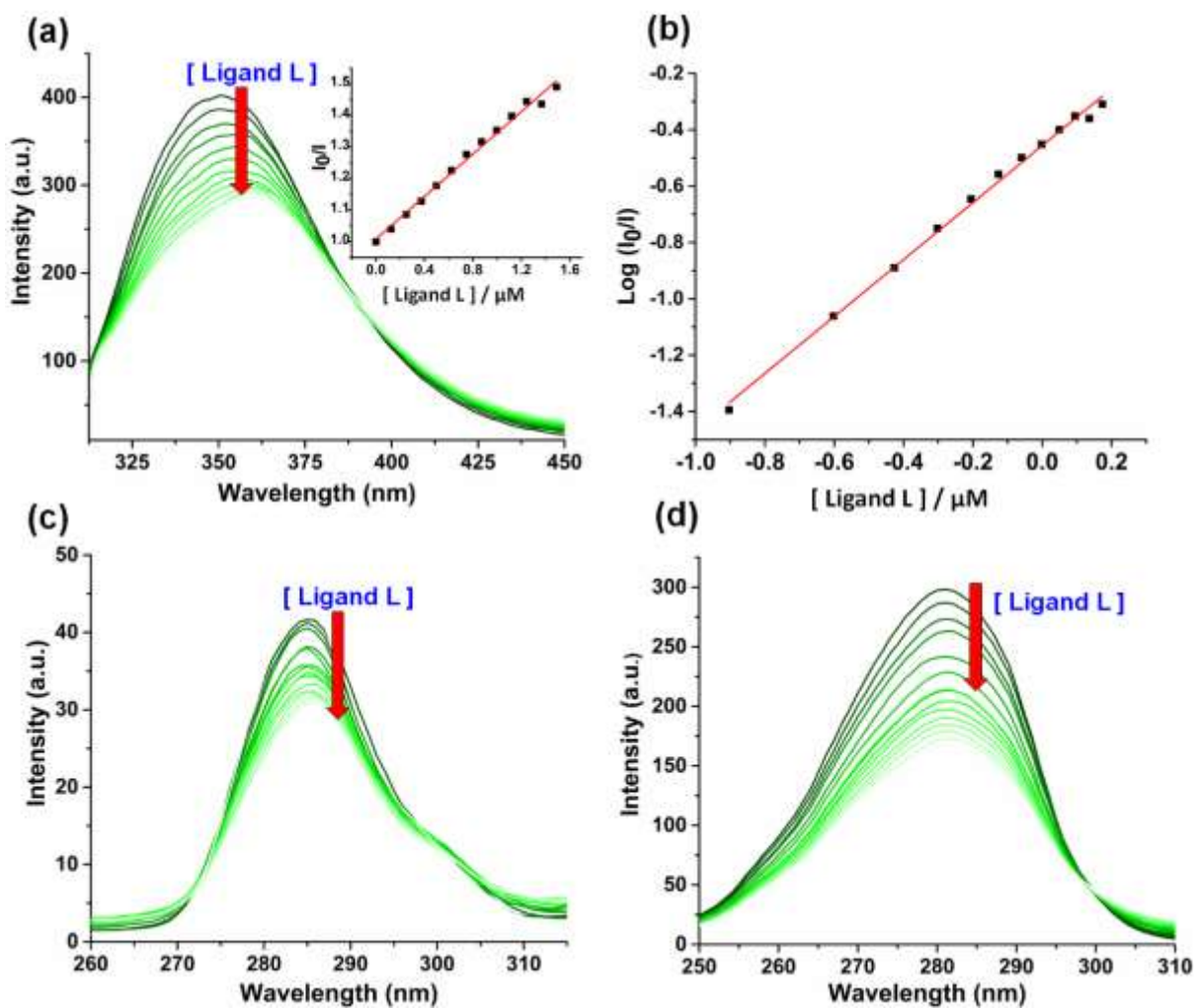


Figure S11. (a) The effect of the addition of [ligand L] in BSA solution in 5 mM Tris buffer (pH 7.2) at 298 K. The inset plot the plot of I_0/I vs. [Ligand L], $\lambda_{ex} = 295$ nm, $\lambda_{em} = 345$ nm, [BSA] = 2 μ M. (b). Modified Stern-Volmer plot of $\log [(I_0 - I)/I]$ vs. \log [Ligand L] for determining the binding constant (K), quenching rate constant (k_q), and the number of binding sites (n) for BSA to the [ligand L] interaction. Emission profile of synchronous emission spectra of BSA showing the quenching of emission after gradual addition of [ligand L] (c) with $\Delta\lambda = 15$ nm and (d) with $\Delta\lambda = 60$ nm in Tris-HCl buffer (pH 7.2) at 298 K.